Abaqus Technology Brief

TB-10-BSTENT-1
Revised: September 2010

Modeling Biodegradable Polymeric Stents Using Abaqus/Standard

Acknowledgement

SIMULIA would like to thank Drs. João S. Soares, James E. Moore, Jr., and Kumbakonam R. Rajagopal. The work presented herein was part of Dr. Soares' doctoral research under professors Moore and Rajagopal at Texas A&M University. Funding was provided by Portuguese Fundação para a Ciência e Tecnologia and the US National Institutes of Health.

Summary

Biodegradable polymeric stents must provide mechanical support of the stenotic artery wall for up to several months while being subjected to cyclic loading that affects the degradation process. To understand the applicability and efficacy of biodegradable polymers, a hyperelastic constitutive model is developed for materials undergoing deformation-induced degradation. The model was implemented in Abaqus/Standard and applied to a commonly used biodegradable polymer system, poly (L-lactic acid) (PLLA).

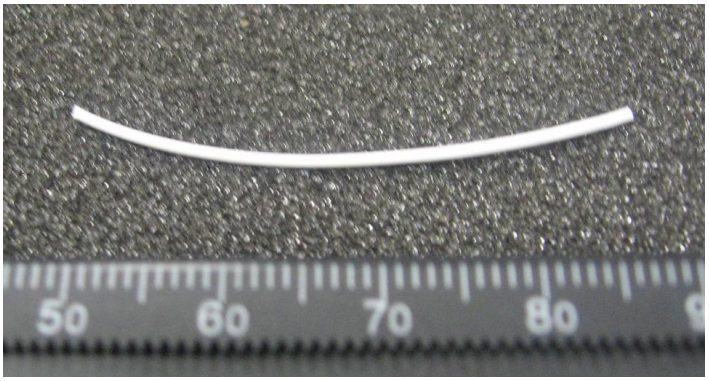

Key Abaqus Features and Benefits

- Ability to include solution-dependent material properties via user subroutine USDFLD
- General capability for defining hyperelastic strain energy potentials with user subroutine UHYPER

Background

Biodegradable stents were introduced on the hypothesis that the need for mechanical support provided by stenting is temporary and is limited to the intervention and shortly thereafter, until re-endothelialization and healing are obtained [1]. Biodegradable polymer stents have several advantageous features: (i) they do not serve as an obstacle for future treatments or a permanent potential nidus for infection; (ii) the gradual softening of the material permits a smooth transfer of the load from the stent to the healing artery, and also contravenes the compliance mismatch between the stent and the stented artery; and (iii) they potentially serve as a reservoir of appreciable size for the incorporation of drugs. The degradation of the stent may play a role in creating optimal drug release kinetics.

The majority of biodegradable polymers used in biomedical applications are synthetic aliphatic polyesters. The prevailing mechanism of degradation of these polymers is random scission by passive hydrolysis when water is present [2], resulting in the commonly observed bulk (or homogeneous) erosion mode [3, 4]. Experimental evidence has shown that deformation and degradation are coupled processes [5-8]. A complete understanding of the interplay between deformation and degradation would be a powerful tool aiding biodegradable stent design. For this purpose, a thermodynamically consistent constitutive description of polymers with deformation-induced degradation was developed [9-11] and employed in the analysis of several stent designs using Abaqus [12]. The goals are to demonstrate the feasibility of incorporating such material models into finite element analysis of stent structures, and to use these models to identify features of biodegradable stent designs that may determine clinical outcomes.

Finite Element Analysis Approach

Constitutive Model

A scalar variable d representing the degree of degradation is first introduced.

$$d = d(\mathbf{x}, t) \tag{1}$$

It measures the degradation of a material particle that is at point $\mathbf{x}$ at time t. The value d = 0 represents a virgin state whereas d = 1 represents the state of maximum degradation. Degradation at a particle, and its consequent reduction of effective crosslinked segments, leads to a reduction of the mechanical properties of that particle.

The stored energy density of the degradable network is a function of the deformation gradient $\mathbf{F}$ and the degree of

degradation,

$$\psi = \psi(\mathbf{F}, d) \tag{2}$$

Material frame indifference and isotropy imply

$$\psi = \psi(I_{\mathbf{B}}, II_{\mathbf{B}}, d) \tag{3}$$

The Cauchy stress is given by

$$\mathbf{T} = -p\mathbf{1} + 2\rho\frac{\partial\psi}{\partial I_{\mathbf{B}}}\mathbf{B} - 2\rho\frac{\partial\psi}{\partial II_{\mathbf{B}}}\mathbf{B}^{\mathrm{T}} \tag{4}$$

where $\mathbf{B} = \mathbf{F}\mathbf{F}^{\mathrm{T}}$, $I_{\mathbf{B}}$ and $II_{\mathbf{B}}$ are the first and second invariants of $\mathbf{B}$. The specific form of the stored energy density, given by

$$\rho\psi(I_{\mathbf{B}}, d) = \lambda(d)e^{-(I_{\mathbf{B}}-3)}(I_{\mathbf{B}}-3) + \mu(d)\ln[1 + a(I_{\mathbf{B}}-3)] \tag{5}$$

was found to provide the best fit for experimental data obtained for PLLA fiber. $\lambda(d)$ and $\mu(d)$ are functions of degradation, whereas a is a material constant. A linear relationship is assumed between degradation and decrease in material properties

$$\lambda(d) = \lambda_0(1-d) \tag{6}$$

$$\mu(d) = \mu_0(1-d) \tag{7}$$

where λ_0 and μ_0 are the virgin state material constants. Deformation-driven degradation is governed by

$$\dot{d} = (1-d)k(\mathbf{F}) \tag{8}$$

where the reaction rate k was chosen to be linear with a scalar measure of deformation, the radius in the ($I_{\mathbf{B}}$, $II_{\mathbf{B}}$) plane:

$$k(\mathbf{F}) = k(I_{\mathbf{B}}, II_{\mathbf{B}}) = \frac{1}{\tau_D}[(I_{\mathbf{B}}-3)^2 + (II_{\mathbf{B}}-3)^2]^{1/2} \tag{9}$$

The constant τ_D is a characteristic time of degradation.

Implementation in Abaqus

Abaqus/Standard allows the definition of solution dependent material properties through the use of field variables; degradation d is incorporated as a field variable. The evolution of degradation is obtained at the beginning of each increment through user subroutine USDFLD, which is used to define solution-dependent field variables at an integration point. Most kinematical quantities are directly available in the subroutine: $I_{\mathbf{B}}$ and $II_{\mathbf{B}}$ can be obtained from $\mathbf{F}$ and once the reaction rate k is determined, Eq.(8) can be integrated numerically yielding d at the end of the increment. A trapezoid integration rule was used for the numerical integration of Eq. (8). After updating the field variables, Abaqus/Standard computes stresses at the end of each increment.

Subroutine UHYPER provides a general capability for defining isotropic hyperelastic materials. Newly updated field variables (in this case d, computed in USDFLD) and kinematical quantities (such as the current values of $I_{\mathbf{B}}$ and $II_{\mathbf{B}}$) are provided to the subroutine, which requires specification of the energy density and the corresponding derivatives with respect to the given invariants (in the current case, given by Eq. (5) and only for $\partial\psi/\partial I_{\mathbf{B}} \neq 0$). Note that for the degradable material defined by Eq. (3), the stored energy density function depends not only on the strain invariants but also on the field variable, the degradation parameter d.

Stent geometries

Two previously proposed stent designs [13, 14], denoted as 2B3 and 1Z1 (Figs. 1 and 2) and a Cypher (Fig. 3) stent (Cordis, Johnson & Johnson, Miami Lakes, FL) were considered in this study.

A constant inward pressure of 1 atm was applied to the expanded stents. One end of the stent was fixed in the axial direction, and in stent designs 2B3 and 1Z1 only one quarter of the full circumferential geometry was modeled (exploiting the symmetry of these designs).

Results

Degradation caused reduction of the mechanical properties in the material, and consequently, all stents lost the ability to withstand a constant load and collapsed inwards. The deformation pattern of biodegradable stents is time-dependent with pronounced changes in performance, qualitatively assessed with overall stent deformation patterns (Figs. 1, 2 and 3) and quantitatively measured as average relative recoil in response to a constant load (Fig. 4).

Furthermore, as the more rigid stent lost its stiffness due to degradation, the constant outer pressurization was responsible for buckling of the structure – the cross-section of the 1Z1 stent, initially circular, assumed an ellipsoidal shape after some degradation (Fig. 2). A similar effect was not observed in the other two designs, as their compliance was clearly greater.

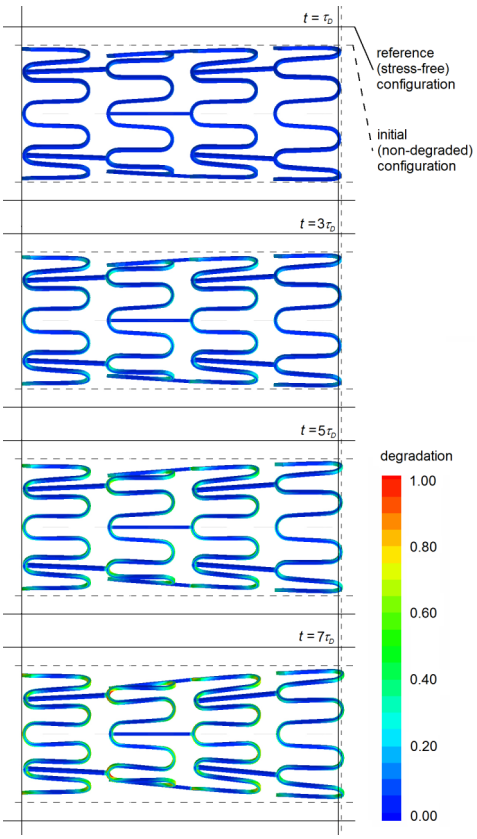

Fig. 1: Degradation of the 2B3 stent [13, 14]. The stent degrad.s mostly at the bends of the rings, where a state of bending prevails, and at their junction points with the connector bars. As the material softens, the stent crept inward under the constant pressure [12].

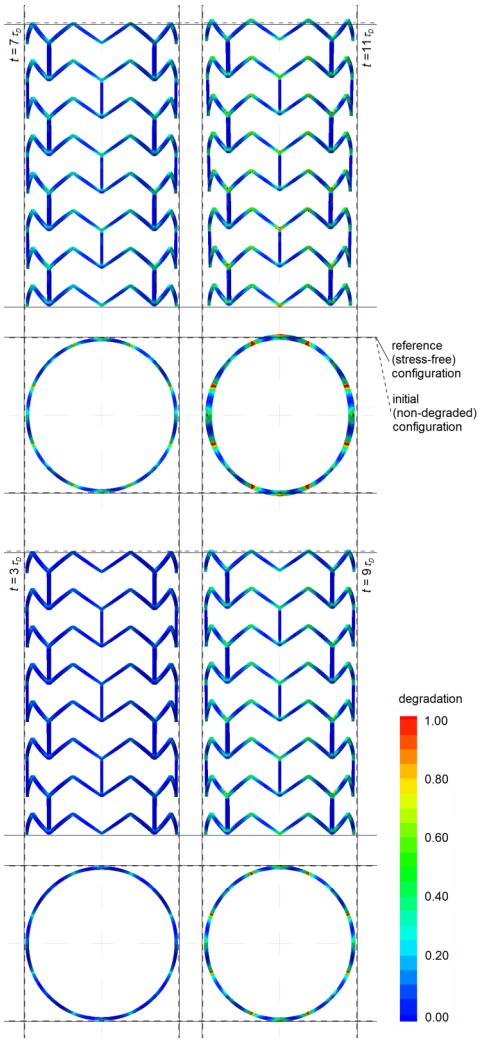

Fig. 2: Degradation of the 1Z1 stent [13, 14] . This design is much stiffer than the 2B3 and much of the deformation and degradation is confined to the junction points and sharp crowns of the stent rings. If failure occurs at these locations, struts that are mostly non-degraded can provoke embolic complications downstream. As the material loses its integrity, buckling of the cylindrical structure is observed to initiate [12].

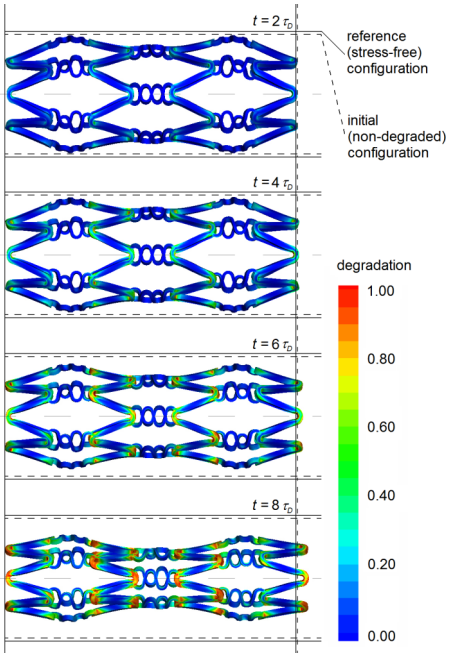

Fig. 3: Degradation of a biodegradable version of the Cypher stent. Degradation occurs dramatically at the junction points due to their complex shape, and the stent loses its stiffness and creeps inwards [12].

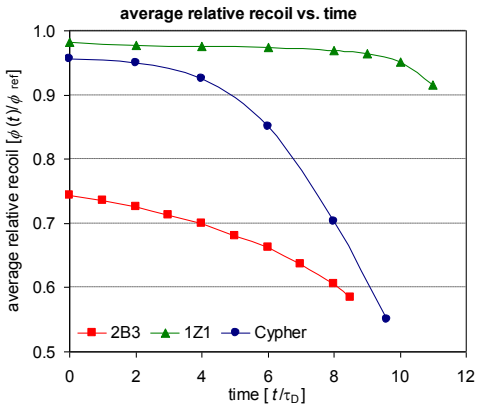

Fig. 4: Average relative recoil vs. time of the different designs subjected to constant outer pressurization [12].

Conclusions

Compared to permanent stents, the study of biodegradable stents is still in its infancy. Many challenges remain in order to fully understand the physics of the material. In this Technology Brief, a hyperelastic constitutive model of a biodegradable polymer, its implementation in Abaqus and application to stent analysis are presented. The capability of Abaqus/Standard to account for the degradation of material properties clearly extends its utility as an analysis tool into the design of biodegradable stents.

References

1. Kastrati, A., Hall, D., and Schomig, A., 2000, *Long-Term Outcome after Coronary Stenting*, Curr Control Trials Cardiovasc med, 1(1):48-54.
2. Weir, N. A., et al., 2004, *Degradation of Poly-L-Lactide: Part 1: In Vitro and in Vivo Physiological Temperature Degradation*, Proceedings of the Institution of Mechanical Engineers Part H-Journal of Engineering in Medicine, 218(H5):307-319.
3. Gopferich, A., 1997, *Handbook of Biodegradable Polymers*, Harwood Academic Publishers, Australia, Mechanisms of Polymer Degradation and Elimination.
4. Burkersroda, F. V., et al., 2002, *Why Degradable Polymers Undergo Surface Erosion or Bulk Erosion*, Biomaterials, 23 (21):4221-4231.
5. Chu, C. C., 1985, *Strain-Accelerated Hydrolytic Degradation of Synthetic Absorbable Sutures*, C. W. Hall, eds., San Antonio, 111-115.
6. Zhong, S. P., et al., 1993, *The Effect of Applied Strain on the Degradation of Absorbable Suture in Vitro*, Clin Mat, 14(3):183-189.
7. Wiggins, M. J., et al., 2003, *Effect of Strain and Strain Rate on Fatigue-Accelerated Biodegradation of Polyurethane*, J Biomed Mater Res A, 66A(3):463-475.
8. Wiggins, M. J., et al., 2004, *Effect of Soft-Segment Chemistry on Polyurethane Biostability During in Vitro Fatigue Loading*, J Biomed Mater Res A, 68A(4):668-683.
9. Rajagopal, K. R., et al., A. S., 2007, *On the Shear and Bending of a Degrading Polymer Beam*, Int J Plasticity, 23(9):1618-1636.
10. Soares, J. S., et al., 2008, *Constitutive Framework for Biodegradable Polymers with Applications to Biodegradable Stents*, ASAIO Journal, 54(3):295-301.
11. Soares, J. S., et al., 2010, *Deformation-Induced Hydrolysis of a Degradable Polymeric Cylindrical Annulus*, Biomech Model Mech, 9(2):177-86
12. Soares, J. S., et al., in press, *Modeling of Deformation-Accelerated Breakdown of Polylactic Acid Biodegradable Stents*, J Med Devices.
13. Bedoya, J., et al., 2006, *Effects of Stent Design Parameters on Normal Artery Wall Mechanics*, J Biomech Eng, 128(5):757-65.
14. Timmins, L. H., et al., 2007, *Stented Artery Biomechanics and Device Design Optimization*, Med Biol Eng Comput, 45(5):505-13.

Abaqus References

For additional information on the Abaqus capabilities referred to in this brief, please see the following Abaqus Version 6.11 documentation references:

- Abaqus User Subroutines Reference Manual
  - Section 1.1.37 “UHYPER”
  - Section 1.1.49 “USDFLD”